Light–Atom Influences on the Electronic Structures of Iron Sulfur Clusters

6 AUTHORS, INCLUDING:

Wei Zhang
University of Waterloo
12 PUBLICATIONS   87 CITATIONS

SEE PROFILE

Kyle M Lancaster
Cornell University
35 PUBLICATIONS   706 CITATIONS

SEE PROFILE

Light-Atom Influences on the Electronic Structures of Iron–Sulfur Clusters

Christopher J. Pollock,[†] Lay Ling Tan,[‡] Wei Zhang,[‡] Kyle M. Lancaster,[§] Sonny C. Lee,*[‡] and Serena DeBeer*[†,§]

[†]Max-Planck-Institut für Chemische Energiekonversion, Stiftstrasse 34-36, D-45470 Mülheim an der Ruhr, Germany

[‡]Department of Chemistry, University of Waterloo, Waterloo, Ontario, Canada N2L3G1

[§]Department of Chemistry and Chemical Biology, Cornell University, Ithaca, New York 14853, United States

S *Supporting Information*

ABSTRACT: Ligand K-edge X-ray absorption spectroscopy was used to study dimeric and tetrameric Cl-terminated Fe–S clusters with variable numbers of S^{2-} substituted by N^tBu^{2-} (N^tBu^{2-} = tertbutylimido) ligands to gain insights into the functional role of the interstitial light atom in the iron–molybdenum cofactor (FeMoco) of nitrogenase. These studies are complemented by time-dependent density functional theory analysis to quantify the relative effects on Fe–S and Fe–Cl bonding. The results show that N^tBu^{2-} substitution dramatically affects the electronic structure of dimeric clusters, while the impact on tetrameric clusters is small. Strong agreement between experiment and theory merited extension of this analysis to hypothetical clusters with S^{2-} substituted by N and C-atom donor ligands as well as FeMoco itself. These results show that very strong electron donors are required to appreciably modulate the electronic structure of tetrameric (or larger) iron sulfur clusters, pointing to a possible role of the central C^{4-} in FeMoco.
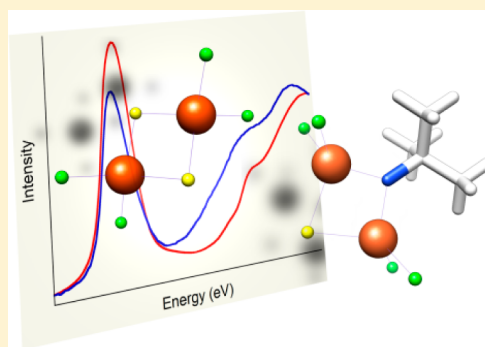
INTRODUCTION

Iron–sulfur clusters are widely dispersed across many metalloprotein families.[1] While these clusters primarily mediate biological electron transfer, many catalytic Fe–S clusters have also evolved. Among the most interesting of these are the M-clusters found in the nitrogenase enzymes that catalyze the eight-electron reduction of N_2 and H^+ to NH_3 and H_2.[2] The most active and best-characterized M-cluster is the iron–molybdenum cofactor (FeMoco), the core of which was recently characterized as Fe_7S_9MoC (Figure 1).[3,4]

This interstitial μ_6-C^{4-} is unique in biology, which engenders the question of what its functional role in the cluster could be. Much biochemical effort goes into the insertion of this carbide. Recently, X-ray emission spectroscopy (XES) measurements showed that the carbide is already present in the Fe_8S_9 "L-

cluster," which is a precursor to the M-cluster.[5] Further, using ^{14}C labeling, Wiig et. al. demonstrated that insertion occurs in a radical *S*-adenosylmethionine-dependent pathway.[6] Naturally, the carbide must exert some influence on the electronic structure of FeMoco, which could have profound implications for the reactivity of nitrogenase.

To explore the effects that a light atom such as carbon has on the electronic structure of Fe–S clusters, we have examined a series of model clusters that have variable numbers of bridging S^{2-} replaced by N^tBu^{2-} (tertbutylimido) groups (Scheme 1). While a C^{4-}-containing model remains elusive, these compounds represent the current highest fidelity structural mimics of the various C^{4-}-containing substructures within FeMoco (Fe_4S_3X root-mean-square deviation (rmsd) = 0.049 Å;[7,8] $Fe_2(\mu_2$-$S)(\mu_2$-$X)$ rmsd = 0.116 Å, where X = C^{4-} in FeMoco and N^tBu^{2-} in the model complexes). Despite being μ_3 (or μ_2) bound rather than μ_6 as in FeMoco, the imide substitutions in these compounds should provide valuable insight into the effects that light-atom substitution has on the electronic structure of Fe–S clusters.

To probe these electronic structure perturbations, we have employed ligand (S and Cl) X-ray absorption spectroscopy (XAS).[9] The pre-edge features observed in these spectra arise due to transitions from the ligand 1s orbitals to unoccupied
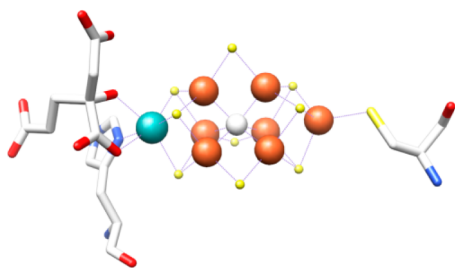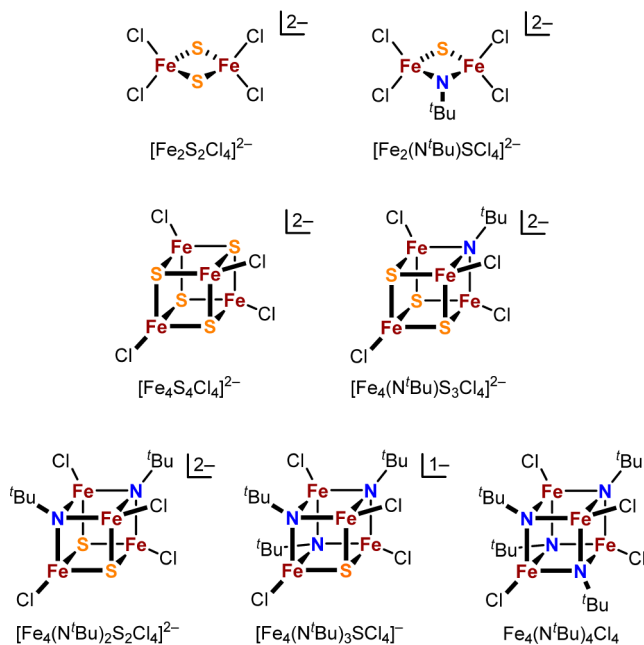

Figure 1. Structure of the nitrogenase iron–molybdenum cofactor.

Scheme 1. Structures of the Compounds Used in This Study

$[Fe_2S_2Cl_4]^{2-}$ $[Fe_2(N^tBu)SCl_4]^{2-}$

$[Fe_4S_4Cl_4]^{2-}$ $[Fe_4(N^tBu)S_3Cl_4]^{2-}$

$[Fe_4(N^tBu)_2S_2Cl_4]^{2-}$ $[Fe_4(N^tBu)_3SCl_4]^-$ $Fe_4(N^tBu)_4Cl_4$

molecular orbitals (MOs) containing ligand 3p character. Thus, as the lowest-lying unoccupied MOs correspond to the partially filled d-manifold, the pre-edge area may be related to the metal−ligand covalency (α^2) via the transition moment dipole integral $I(S) = \langle S_{1s}|\vec{r}|S_{3p}\rangle$. Using this relationship, ligand K-edge XAS has afforded much insight into the electronic structure of diverse Fe−S clusters and their dependences on redox state, surrounding protein matrix, and solvation.[10−14]

To complement our experimental studies, we have used time-dependent density functional theory (TD-DFT) to calculate XAS pre-edge spectra. Spectra calculated using TD-DFT have been shown to reproduce experiment extremely well[15−18] and can be used to correlate experimental areas to ligand 3p character, thus allowing determination of $I(S)$.[19,20] Importantly, this approach calculates the oscillator strength and thus allows for a more direct correlation of experimental areas with covalency in a manner that mitigates uncertainty associated with experimentally estimating the dipole integral. The spectra calculated for the compounds studied herein reproduce the experimental trends quite well and are extended

to hypothetical clusters containing N- and C-atom substituents as well as FeMoco itself to better understand the effect of the central carbide on the electronic structures of large clusters such as FeMoco.

■ EXPERIMENTAL SECTION

Sample Preparation. All clusters were prepared according to literature methods.[7,8,21−23] After synthesis, compounds were stored in a glovebox under a N_2 atmosphere.

XAS Measurements. All XAS spectra were collected at the Stanford Synchrotron Radiation Lightsource beamline 4−3 (20 pole wiggler) under ring conditions of 3 GeV and 350 mA. Samples were prepared in a nitrogen atmosphere glovebox by grinding to a fine powder with boron nitride and were dispersed as thinly as possible onto 38 μm Kapton tape. A window of 5 μm polypropylene film was placed over the samples to prevent exposure to air. All samples were measured in a He atmosphere at room temperature with a Lytle detector in fluorescence mode. Data represent an average of 2−3 scans collected between 2420 and 2720 eV (S) or 2815 and 2865 eV (Cl). The incident beam energy was calibrated for S using the spectrum of $Na_2S_2O_3\cdot5\ H_2O$ (2472.02 eV) and for Cl using the spectrum of Cs_2CuCl_4 (2820.20 eV). Intensity was normalized with respect to the incident beam using a He-filled ion chamber upstream of the sample.

Data Processing. Data were processed using EXAFSPAK[24] and fit using BlueprintXAS.[25] A pre-edge background was subtracted from all spectra by fitting a polynomial to the pre-edge region and then subtracting this function from the entire spectrum; postedge backgrounds (linear or quadratic) were fit during peak fitting and subsequently subtracted. Peak positions and areas were found by fitting pseudo-Voigt peaks to the pre-edge and near edge regions of the data. Where possible, second derivatives were used as guides to determine the energy position and number of pre-edge peaks. In cases where the noise level of the second derivative prohibited such an approach, peaks were sequentially added to the fit until no further statistical improvement in the goodness of fit was achieved. Reported values represent an average of at least 15 reasonable fits, as judged by the sum of squares due to error (SSE) parameter. For all compounds, all fit peaks falling at or below 2471.2 eV were included in the pre-edge areas. Spectra were normalized by setting the edge jump equal to 1. For spectra that showed evidence of sulfate and/or sulfonate contamination, reference spectra of K_2SO_4 and CH_3SO_3Na were fit to the data as well, and the contributions of these spectra to the edge jump were removed before normalization. In no case did contamination interfere with analysis or represent more than 15% of the total signal.

Computations. All calculations were performed using the ORCA 2.9 quantum chemical suite.[26] Geometry optimizations used crystal structures as starting coordinates and were performed using the BP86
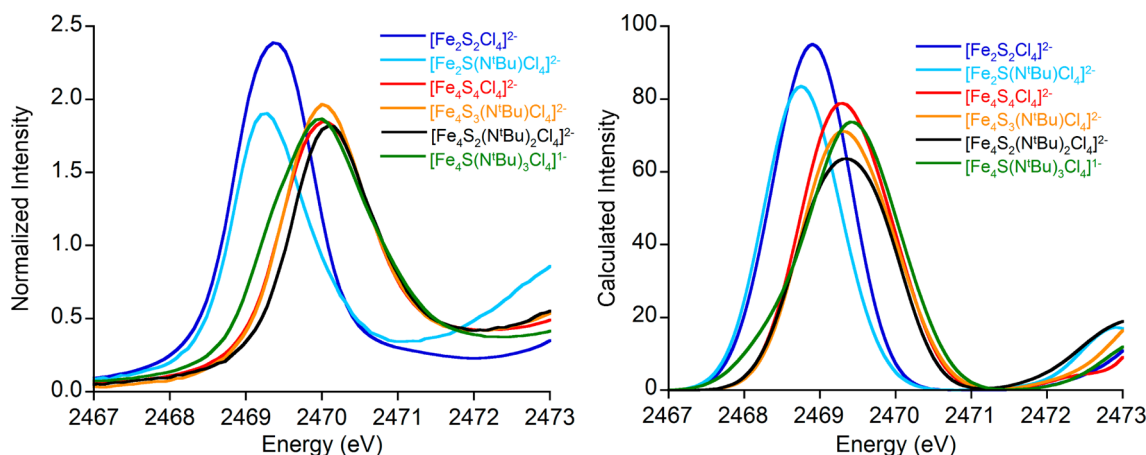

Figure 2. (left) The experimental S pre-edges. (right) The TD-DFT calculated spectra.

Table 1. Analysis of S K-Edge XAS Data

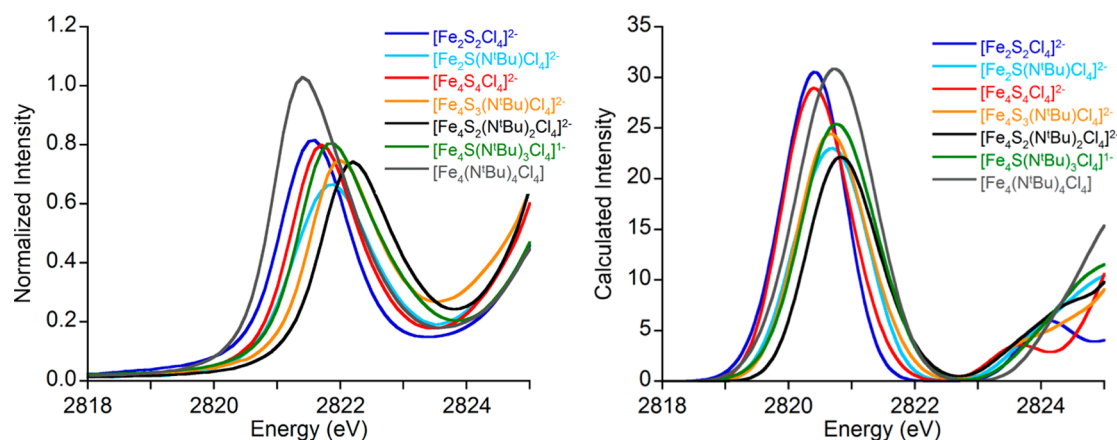|	pre-edge area	$f_{osc} \times 10^4$ (calculated)	% S p (calculated)
$[Fe_2S_2Cl_4]^{2-}$	3.87 ± 0.18	42.08	81.3%
$[Fe_2S(N^tBu)Cl_4]^{2-}$	2.87 ± 0.13	36.64	73.3%
$[Fe_4S_4Cl_4]^{2-}$	3.15 ± 0.24	40.08	69.5%
$[Fe_4S_3(N^tBu)Cl_4]^{2-}$	3.01 ± 0.22	36.84	67.3%
$[Fe_4S_2(N^tBu)_2Cl_4]^{2-}$	3.01 ± 0.33	33.97	62.8%
$[Fe_4S(N^tBu)_3Cl_4]^{1-}$	3.70 ± 0.14	41.15	73.9%

Figure 3. (left) The experimental Cl pre-edges. (right) The TD-DFT calculated spectra.

functional[27,28] and the def2-TZVP(-f) basis set.[29] Solvation was modeled using the conductor-like screening model (COSMO)[30] with a dielectric of 9.08 (CH_2Cl_2). Metrical parameters for all geometry-optimized structures can be found in Supporting Information, Table S1. While the compounds studied all exhibit magnetic coupling between the various high-spin Fe centers, all optimizations were performed using the high-spin state (all unpaired spins parallel). S and Cl pre-edges were calculated using TD-DFT as described previously.[15,18,31] Because of uncertainties in the spin coupling in these systems, single-point energies were calculated for all possible broken symmetry solutions, and the lowest-energy solution was used for TD-DFT calculations. Hypothetical clusters were modeled by modifying the N^tBu^{2-} substituent in geometry-optimized $[Fe_4S_3(N^tBu)Cl_4]^{2-}$ as needed, followed by geometry optimization. Spin coupling was assumed to be the same as in the parent cluster. Calculations on FeMoco were performed using a 55 atom model based on a previously geometry-optimized structure and spin-coupling scheme—this model incorporated the $MoFe_7S_9X$ core along with the bound histidine, cysteine, and homocitrate ligands and an overall charge of −3.[3] For N- and O-substituted clusters, the central carbide was replaced by the desired atom without further optimization. For all compounds, spectra were calculated for each absorbing atom and then averaged together to obtain a total spectrum. A dense integration grid was used for all calculations (ORCA Grid4). Calculated spectra were plotted using 1 eV fwhm broadening and were shifted by constants of 76.25 and 85.3 eV (for S and Cl, respectively) to match experiment.[15,18] Reported oscillator strengths were obtained by summing the individual f_{osc} values for all calculated pre-edge transitions. Covalency values were obtained by summing the S/Cl 3p character over the unoccupied d-orbitals (based on Löwdin population analysis of the canonical orbitals). Orbitals and difference density plots were visualized using Chimera.[32]

■ RESULTS AND ANALYSIS

Ligand K-Edge XAS. Pre-edges from the S K-edge XAS spectra of the dinuclear and tetranuclear clusters are presented along with the corresponding DFT-calculated spectra in Figure 2; fitting parameters are presented in Table 1, and the fits themselves can be found in Figures S1 and S2 in the Supporting

Information. These spectra have been normalized to an edge jump of unit intensity, so intensities presented correspond to the average value per sulfur.

For the dimeric clusters, significant pre-edge intensity is lost on going from $[Fe_2S_2Cl_4]^{2-}$ to $[Fe_2S(N^tBu)Cl_4]^{2-}$, indicating decreased S 3p contribution to the metal valence orbitals. As N^tBu^{2-} is expected to be a very effective σ-donor, its ability to outcompete the contribution from S^{2-} is perhaps not surprising. While a similar effect might be expected for the tetrameric clusters, this is not in fact realized experimentally. Indeed, within experimental error, all of the isoelectronic tetramers have equivalent pre-edge areas. (An increase in pre-edge intensity is seen for $[Fe_4S(N^tBu)_3Cl_4]^{1-}$ owing to an additional d-manifold hole in this more oxidized complex.) This observation suggests that, while N^tBu^{2-} substitution has a significant impact upon the electronic structures of the dimers, its effects on the tetramers are minimal. Energetically, substitution has little effect on any of the compounds studied, though a consistent shift of 0.5 eV to higher energy is seen for the tetramers relative to the dimers.

The TD-DFT calculated pre-edges largely reproduce these experimental trends. Substituting S^{2-} with N^tBu^{2-} in the dimers results in a noticeable decrease in pre-edge oscillator strength (Table 1), though the calculations appear to slightly under-estimate this effect. Further, the shift to higher energy for the tetrameric cluster pre-edges is also reproduced and can be attributed to slightly greater stabilization of the $\mu_3\text{-}S^{2-}$ 1s orbitals over those of the $\mu_2\text{-}S^{2-}$. Contrary to the experimental results, however, the calculated pre-edges for the tetramers do, in fact, show a small, consistent loss of intensity with N^tBu^{2-} substitution. The effect is small—roughly a 15% change in the calculated f_{osc} between $[Fe_4S_4Cl_4]^{2-}$ and $[Fe_4S_2(N^tBu)_2Cl_4]^{2-}$—which may indicate that these changes are simply within the margins of experimental error. This is an important point to stress as it serves as a note of caution on the

Table 2. Analysis of Cl K-Edge XAS Data

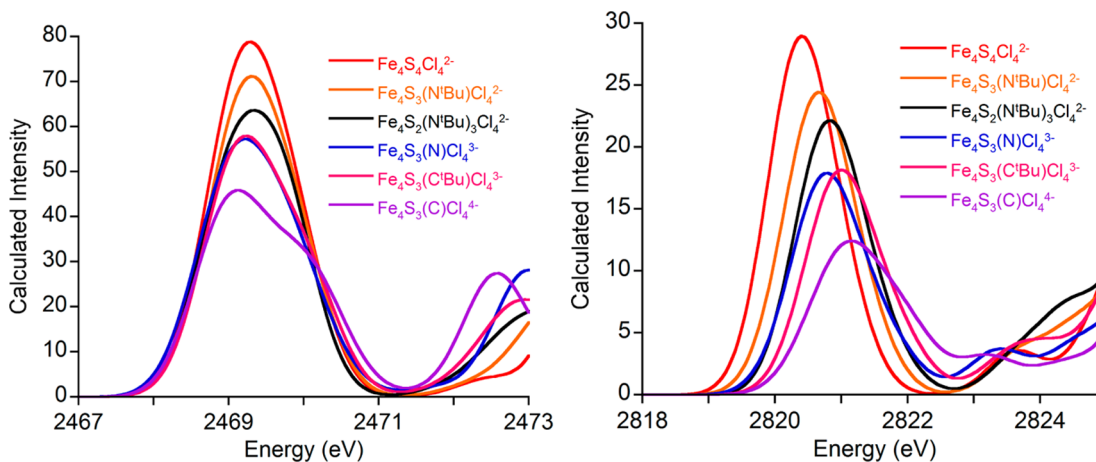|	pre-edge area	$f_{osc} \times 10^4$ (calculated)	% Cl p (calculated)
$[Fe_2S_2Cl_4]^{2-}$	1.43 ± 0.07	13.35	21.2%
$[Fe_2S(N^tBu)Cl_4]^{2-}$	1.12 ± 0.09	11.36	18.4%
$[Fe_4S_4Cl_4]^{2-}$	1.26 ± 0.03	13.49	21.2%
$[Fe_4S_3(N^tBu)Cl_4]^{2-}$	1.17 ± 0.08	11.86	19.4%
$[Fe_4S_2(N^tBu)_2Cl_4]^{2-}$	1.20 ± 0.06	10.85	17.6%
$[Fe_4S(N^tBu)_3Cl_4]^{1-}$	1.44 ± 0.07	13.15	21.3%
$[Fe_4(N^tBu)_4Cl_4]$	1.79 ± 0.11	16.59	25.6%

Figure 4. Calculated pre-edges for hypothetical clusters with nitride, alkylidyne, and carbide substitutions. (left) S. (right) Cl.

Table 3. Calculated Parameters for Hypothetical Clusters

	S $f_{osc} \times 10^4$ (calculated)	% S p (calculated)	Cl $f_{osc} \times 10^4$ (calculated)	% Cl p (calculated)
$[Fe_4S_4Cl_4]^{2-}$	40.08	69.5%	13.49	21.2%
$[Fe_4S_3(N^tBu)Cl_4]^{2-}$	36.84	67.3%	11.86	19.4%
$[Fe_4S_2(N^tBu)_2Cl_4]^{2-}$	33.97	62.8%	10.85	17.6%
$[Fe_4S_3(N)Cl_4]^{3-}$	33.08	62.0%	9.40	15.1%
$[Fe_4S_3(C^tBu)Cl_4]^{3-}$	32.55	61.4%	9.41	14.9%
$[Fe_4S_3(C)Cl_4]^{4-}$	29.50	57.5%	7.49	11.8%

quantitative accuracy of covalency numbers extracted from experimental data.

These calculations afford insights into the origins of the effects seen upon light-atom substitution. Analysis of the metrical parameters reveals that, for both the dimers and the tetramers, the Fe−S bond lengths remain essentially unchanged upon substitution (Supporting Information, Table S1), indicating the loss of pre-edge intensity results almost exclusively from electronic rather than from geometric perturbations. For isoelectronic compounds, N^tBu^{2-} substitution results in decreased S p mixing into the valence orbitals (Table 1), demonstrating that, as expected, these strongly donating groups outcompete the contribution from S^{2-}. A closer examination of the dimers is provided in Supporting Information, Table S3, where the electronic origins of the observations are discussed. Furthermore, the calculations confirm that replacement of a single S^{2-} with N^tBu^{2-} has a much larger effect on S participation in bonding for the dimers (8% reduction) as compared to the tetramers (2.2% and 4.5% reductions).

This same analysis can be employed for the Cl K-edge XAS data (Figure 3, Table 2). Again, for the dimeric compounds, substitution of S^{2-} for N^tBu^{2-} results in a significant decrease in pre-edge intensity, demonstrating that the terminal atoms as

well as bridging atoms in Fe−S clusters are impacted by light-atom substitution. An energetic shift of roughly 0.2 eV to higher energy is also observed, consistent with increased destabilization of the ligand field manifold. As also seen for the S XAS data, within experimental error the isoelectronic tetrameric clusters do not show any consistent trend in pre-edge intensities, though each successive substitution does increase the pre-edge energy by roughly 0.2 eV. Unlike the bonds to S, the Fe−Cl bonds do show modest changes (0.03 Å elongation) upon substitution (Supporting Information, Table S1) that match the experimentally observed trend,[8] though this does not appear to be observable in the data. The more oxidized clusters show greater pre-edge areas (and shorter Fe−Cl bonds) due to the presence of additional holes in the d-manifolds of these complexes. DFT calculations generally reproduce these effects, though again a consistent decrease in pre-edge oscillator strength is calculated with increasing N^tBu^{2-} substitution. We attribute the lack of an apparent experimental effect to the inherent uncertainties involved in the fitting and normalization procedure employed.

DFT Calculations of Hypothetical Clusters. From the experimental results, it is clear that light-atom substitution perturbs the electronic structures of dimeric Fe−S clusters; for tetramers, however, it is difficult to discern any effect outside

experimental uncertainty. To expand our understanding of how this substitution affects the electronic structures of these clusters, we have computationally investigated hypothetical clusters where S^{2-} ligands have been replaced by the even stronger donors N^{3-}, C^tBu^{3-}, and C^{4-} (Figure 4, Table 3). The limits of this series (S^{2-}) and (C^{4-}) thus take a step toward understanding the difference between a typical iron−sulfur cluster and a "light-atom modified" iron−sulfur cluster such as that found in FeMoco. Calculations on the full FeMoco cluster are explored in the section that follows.

The computations on these hypothetical clusters confirm that these exceptionally strong donors attenuate S and Cl participation to a much greater extent than does N^tBu^{2-}, consistent with their being even more effective charge donors. Relative to the unsubstituted $[Fe_4S_4Cl_4]^{2-}$ cluster, the nitride and carbide substitutions result in 17% and 26% reductions in sulfur pre-edge intensity, respectively, much greater than what is observed for a single imide substitution (∼8%). Even more dramatic are the computational results for Cl, which predict a 44% decrease in pre-edge intensity upon carbide substitution. Proportional reductions in S and Cl orbital mixing are also seen: substituting a sulfide for a carbide, for example, reduces S character from 69.5% to 57.5% and Cl character from 21.2% to 11.8%. Pre-edges for both ligands also show a redistribution of intensity to slightly higher energies, especially for the carbide-substituted cluster, consistent with increasing ligand-field destabilization.[9]

Lastly, the effect of charge versus light-atom identity was investigated by comparing the latter two compounds to one with a C^tBu^{3-} substitution. Although the donor atom for the alkylidyne ligand is a carbon, the calculated pre-edges for this cluster much more closely resemble those for the charge-equivalent nitride, revealing that—for similar light-atom substituents—the charge on the donor plays a dominant role in electronic structure perturbation.

These computational results further support the observation that light-atom donors perturb the electronic structures of Fe−S clusters but that only very strong electron donors were seen to appreciably influence the electronics of larger clusters. Together, these observations indicate that electronic structure modulation may be one role played by the central carbide in the Fe_7Mo FeMoco cluster.

DFT Calculations on FeMoco. To test these predictions, calculations were carried out on computational models of the FeMoco active site with C, N, and O as the interstitial atom ($FeMoco^C$, $FeMoco^N$, and $FeMoco^O$, respectively). The predicted S K-edges are shown in Figure 5, and the calculated

covalencies are shown in Table 4. We note that the calculated pre-edge at ∼2470 eV is consistent with the published S K-edge

Table 4. Calculated FeMoco Parameters

	% S p	% C/N/O s + p
$FeMoco^C$	67.6	132.0
$FeMoco^N$	69.2	110.3
$FeMoco^O$	72.6	75.4

data on FeMoco.[33] Unfortunately, a more quantitative analysis of these data is not possible as the presence of excess dithionite, required to stabilize the resting form, precludes a quantitative analysis of these data.

The prediction that a very strong donor, such as the central carbide, would have an impact on the electronic structure of a large cluster is supported by these computations, with a 5% decrease in S contribution to the valence d orbitals between $FeMoco^O$ and $FeMoco^C$. This reduction is comparable to the changes seen between the $[Fe_4S_4Cl_4]^{2-}$ and $[Fe_4S_2(N^tBu)_2Cl_4]^{2-}$ tetramers (6.7%). Furthermore, the experimental observation that the terminal atoms are impacted more than the bridging atoms is reproduced in the cubane subunits of FeMoco, as shown in Supporting Information, Table S4, where it can be seen that the μ_2-sulfides show a much greater reduction in intensity than the corresponding μ_3 or cysteine sulfurs.

Perhaps not surprisingly, the calculated decrease in pre-edge intensity between oxide and carbide is relatively small and is unlikely to be distinguishable experimentally at current resolutions. Given the differential changes between μ_2- and μ_3-S^{2-} (Supporting Information, Table S4), however, these subtle variations may be observable at improved experimental resolution that better approaches the limit imposed by the S 1s core hole lifetime.

■ DISCUSSION

Substitution of S^{2-} for light-atom donors has been shown to impact the electronic structures of Fe−S clusters. These effects were attributed to the increased charge-donation ability of the light-atom substituents, an argument which has also been invoked to contrast μ_2- versus μ_3-S^{2-} coordination.[13] For dimers, replacement of a single sulfide for N^tBu^{2-} greatly reduces both S and Cl participation in bonding; the electronics of tetramers, however, are not significantly perturbed by even two N^tBu^{2-} groups. Computationally, even stronger donors were investigated, and these were shown to have a more pronounced effect on the tetrameric clusters—for singly substituted clusters, the order of charge donation effectiveness is $S^{2-} < N^tBu^{2-} < N^{3-} \approx C^tBu^{3-} < C^{4-}$—indicating that only very strong donors managed to impact the electronic structures of larger Fe−S clusters.

The enhanced charge donation associated with strongly basic light-atom substituents increases electron density on both the Fe centers and the remaining S^{2-} ligands, leading to a number of potential impacts on the properties of these clusters. As can already be seen for the tetranuclear cubanes, substitution of S^{2-} for N^tBu^{2-} lowers the 2−/3− reduction potentials by ∼400 mV each,[7,8] and it can be expected that substitution by N^{3-} or C^{4-} would have an even greater impact. This argument readily applies to FeMoco, as well. The experimentally determined potential of −0.042 V versus normal hydrogen electrode for the oxidation of resting FeMoco[34] has been used to evaluate
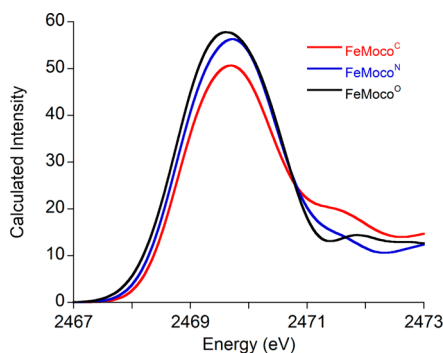
Figure 5. TD-DFT calculated S K-edge spectra for FeMoco models with varying interstitial atoms.

electronic structure solutions of the cofactor with variable central atoms and oxidation state distributions. The calculated reduction potentials in these analyses are 0.8−1.5 V lower for FeMoco[C] relative to the FeMoco[N] when Fe oxidation state and homocitrate protonation are kept constant.[35,36] For FeMoco[C] to exhibit a similar reduction potential to FeMoco[N], it must possess a higher complement of Fe[III], demonstrating that the central C[4−] is sufficient to influence the electronic structure of the cluster. These results are supported by our own calculations on FeMoco, which showed appreciable differences in S contribution between FeMoco[C] and FeMoco[N]/FeMoco[O].

Of course, it should be noted that the light-atom substituents studied here were μ_3 (or μ_2 for the dimers), while the central atom of FeMoco is μ_6. Hence, any effect exerted by the carbide in FeMoco would be distributed over a cluster that is twice the size of those studied here. This supposition is borne out by the observation that the reduction induced by carbide substitution on the tetramers (12%) is roughly twice that seen with FeMoco (5%). Admittedly, this is an imperfect comparison as the starting compounds begin with sulfide and oxide donors, respectively, though the differences are still illuminating.

Even in a μ_6 environment, the changes seen upon C[4−] substitution support the proposition that, despite charge delocalization across a larger cluster, the central carbide is still able to influence the electronics of a cofactor like FeMoco. The impact the electronic structure has on the reactivity of the cofactor awaits further experimental investigation. However, the present study suggests that the C[4−] in FeMoco, in addition to its structural role, exerts a significant electronic influence over the cluster. The nature of this influence and its implications for N_2 fixation are under investigation in our laboratory.

■ ASSOCIATED CONTENT

ⓢ Supporting Information
Representative fits to XAS data for S and Cl K-edges for each compound, diagrams of orbital contributions for dimer S XAS calculations, breakdown of sulfur contributions for FeMoco calculations, metrical parameters for geometry optimized clusters, sample ORCA input files for optimization, broken symmetry, and TD-DFT calculations, optimized *xyz* coordinates for all structures, lowest-energy broken-symmetry coupling schemes for each compound. This material is available free of charge via the Internet at http://pubs.acs.org.

■ AUTHOR INFORMATION

Corresponding Authors
*E-mail: serena.debeer@cec.mpg.de (S.D.).
*E-mail: sclee@uwaterloo.ca (S.C.L.).

Notes
The authors declare no competing financial interest.

■ ACKNOWLEDGMENTS

■ REFERENCES

(1) Beinert, H.; Holm, R. H.; Münck, E. *Science* **1997**, *277*, 653−659.
(2) Hu, Y.; Ribbe, M. W. *Acc. Chem. Res.* **2010**, *43*, 475−484.
(3) Lancaster, K. M.; Roemelt, M.; Ettenhuber, P.; Hu, Y.; Ribbe, M. W.; Neese, F.; Bergmann, U.; DeBeer, S. *Science* **2011**, *334*, 974−977.
(4) Spatzal, T.; Aksoyoglu, M.; Zhang, L.; Andrade, S. L. A.; Schleicher, E.; Weber, S.; Rees, D. C.; Einsle, O. *Science* **2011**, *334*, 940.
(5) Lancaster, K. M.; Hu, Y.; Bergmann, U.; Ribbe, M. W.; DeBeer, S. *J. Am. Chem. Soc.* **2013**, *135*, 610−612.
(6) Wiig, J. A.; Hu, Y.; Lee, C. C.; Ribbe, M. W. *Science* **2012**, *337*, 1672−1675.
(7) Chen, X.-D.; Duncan, J. S.; Verma, A. K.; Lee, S. C. *J. Am. Chem. Soc.* **2010**, *132*, 15884−15886.
(8) Chen, X.-D.; Zhang, W.; Duncan, J. S.; Lee, S. C. *Inorg. Chem.* **2012**, *51*, 12891−12904.
(9) Glaser, T.; Hedman, B.; Hodgson, K. O.; Solomon, E. I. *Acc. Chem. Res.* **2000**, *33*, 859−868.
(10) Dey, A.; Glaser, T.; Moura, J. J. G.; Holm, R. H.; Hedman, B.; Hodgson, K. O.; Solomon, E. I. *J. Am. Chem. Soc.* **2004**, *126*, 16868−16878.
(11) Dey, A.; Glaser, T.; Couture, M. M. J.; Eltis, L. D.; Holm, R. H.; Hedman, B.; Hodgson, K. O.; Solomon, E. I. *J. Am. Chem. Soc.* **2004**, *126*, 8320−8328.
(12) Dey, A.; Jenney, F. E.; Adams, M. W. W.; Babini, E.; Takahashi, Y.; Fukuyama, K.; Hodgson, K. O.; Hedman, B.; Solomon, E. I. *Science* **2007**, *318*, 1464−1468.
(13) Glaser, T.; Rose, K.; Shadle, S. E.; Hedman, B.; Hodgson, K. O.; Solomon, E. I. *J. Am. Chem. Soc.* **2001**, *123*, 442−454.
(14) Glaser, T.; Bertini, I.; Moura, J. J. G.; Hedman, B.; Hodgson, K. O.; Solomon, E. I. *J. Am. Chem. Soc.* **2001**, *123*, 4859−4860.
(15) DeBeer George, S.; Neese, F. *Inorg. Chem.* **2010**, *49*, 1849−1853.
(16) Ray, K.; DeBeer George, S.; Solomon, E. I.; Wieghardt, K.; Neese, F. *Chem.—Eur. J.* **2007**, *13*, 2783.
(17) Sproules, S.; Weyhermüller, T.; Goddard, R.; Wieghardt, K. *Inorg. Chem.* **2011**, *50*, 12623−12631.
(18) DeBeer George, S.; Petrenko, T.; Neese, F. *Inorg. Chim. Acta* **2008**, *361*, 965−972.
(19) Sarangi, R.; DeBeer George, S.; Rudd, D. J.; Szilagyi, R. K.; Ribas, X.; Rovira, C.; Almeida, M.; Hodgson, K. O.; Hedman, B.; Solomon, E. I. *J. Am. Chem. Soc.* **2007**, *129*, 2316−2326.
(20) Szilagyi, R. K.; Lim, B. S.; Glaser, T.; Holm, R. H.; Hedman, B.; Hodgson, K. O.; Solomon, E. I. *J. Am. Chem. Soc.* **2003**, *125*, 9158−9169.
(21) Do, Y.; Simhon, E. D.; Holm, R. H. *Inorg. Chem.* **1983**, *22*, 3809−3812.
(22) Wong, G. B.; Bobrik, M. A.; Holm, R. H. *Inorg. Chem.* **1978**, *17*, 578−584.
(23) Verma, A. K.; Nazif, T. N.; Achim, C.; Lee, S. C. *J. Am. Chem. Soc.* **2000**, *122*, 11013−11014.
(24) George, G. N. *EXAFSPAK, EXAFSPAK, SSRL, SLAC*; Stanford University: Stanford, CA.
(25) Delgado-Jaime, M. U.; Mewis, C. P.; Kennepohl, P. *J. Synchrotron Radiat.* **2010**, *17*, 132−137.
(26) Neese, F. *Wiley Interdisciplinary Reviews: Computational Molecular Science*; **2012**, *2*, 73−78.
(27) Becke, A. D. *Phys. Rev. A: At., Mol., Opt. Phys.* **1988**, *38*, 3098.
(28) Perdew, J. P. *Phys. Rev. B* **1986**, *33*, 8822.
(29) Pantazis, D. A.; Chen, X. Y.; Landis, C. R.; Neese, F. *J. Chem. Theory Comput.* **2008**, *4*, 908−919.
(30) Klamt, A.; Schüürmann, G. *J. Chem. Soc., Perkin. Trans.* **1993**, *2*, 799−805.
(31) Ray, K.; George, S. D.; Solomon, E. I.; Wieghardt, K.; Neese, F. *Chem.—Eur. J.* **2007**, *13*, 2783−2797.
(32) Pettersen, E. F.; Goddard, T. D.; Huang, C. C.; Couch, G. S.; Greenblatt, D. M.; Meng, E. C.; Ferrin, T. E. *J. Comput. Chem.* **2004**, *13*, 1605−1612.

(33) Hedman, B.; Frank, P.; Gheller, S. F.; Roe, A. L.; Newton, W. E.; Hodgson, K. O. *J. Am. Chem. Soc.* **1988**, *110*, 3798−3805.

(34) O'Donnell, M. J.; Smith, B. E. *Biochem. J.* **1978**, *173*, 831−838.

(35) Harris, T. V.; Szilagyi, R. K. *Inorg. Chem.* **2011**, *50*, 4811−4824.

(36) Lovell, T.; Liu, T.; Case, D. A.; Noodleman, L. *J. Am. Chem. Soc.* **2003**, *125*, 8377−8383.